Bioorganic Chemistry 142 (2024) 106932

Contents lists available at ScienceDirect

Bioorganic Chemistry

journal homepage: www.elsevier.com/locate/bioorg

Discovery of novel tetrahydrobenzothiophene derivatives as MSBA inhibitors for antimicrobial agents

Shuchen Pei [a,*], Lin Lai [a], Wanlin Sun [a], Zhaoyang Lu [a], Jielei Hao [a], Yuheng Liu [c,d], Wen Wu [b,*], Shan Guan [c,*], Xiaoyan Su [a]

[a] College of Chemistry and Chemical Engineering, Chongqing University of Science and Technology, Chongqing 401331, PR China
[b] Chongqing Key Laboratory of High Active Traditional Chinese Drug Delivery System, Chongqing Engineering Research Center of Pharmaceutical Sciences, Chongqing Medical and Pharmaceutical College, Chongqing 404120, PR China
[c] National Engineering Research Center of Immunological Products, Third Military Medical University, Chongqing 400038, PR China
[d] Department of Pharmacology, College of Pharmacy, Chongqing Medical University, Chongqing 400016, PR China

ARTICLE INFO

Keywords:
Tetrahydrobenzothiophene
Antibacterial
Drug desigen
Synthesis

ABSTRACT

The incidence of infections caused by drug-resistant bacteria has been one of the most serious health threats in the past and is substantially increasing in an alarming rate. Therefore, the development of new antimicrobial agents to combat bacterial resistance effectively is urgent. This study focused on the design and synthesis of 40 novel tetrahydrobenzothiophene amide/sulfonamide derivatives and their antibacterial activities were evaluated. Compounds **2p**, **6p**, and **6 s** exhibited significant inhibitory effects on the growth of bacteria. To assess their safety, the cytotoxicity of the compounds was assessed using human normal liver cells, revealing that compound **6p** has lower cytotoxicity. A mouse wound healing experiment demonstrated that compound **6p** effectively improved wound infection induced by trauma and accelerated the healing process. Compound **6p** holds promise as a potential therapeutic agent for combating bacterial infections.

1. Introduction

For the last few decades, the overuse of antibiotics has given rise to highly resistant and infectious superbugs [1–6]. These superbugs include examples such as methicillin-resistant Staphylococcus aureus (MRSA), drug-resistant tuberculosis bacteria, and drug-resistant Streptococcus pneumoniae [7–14]. These antibiotic-resistant superbugs pose a significant threat to human health as they have developed resistance to most available antibiotics [15–18]. Therefore, there is an urgent need for novel antimicrobial agents to address this challenge.

In spite of some difficulties, researchers have made significant progress in developing various antimicrobial agents to combat drug-resistant bacteria and superbugs. For example, β-lactamase inhibitors like avibactam and vaborbactam can target specific strains resistant to multiple drugs, although they may cause adverse reactions such as nausea, diarrhea, or rash [19,20]. Protein inhibitors like ubiquitin can disrupt bacterial metabolism and exhibit broad-spectrum antibacterial activity but may also trigger allergic reactions or toxic effects in some individuals [21]. Lysozyme shows selectivity and efficiency by disrupting bacterial cell walls. However, they may also face resistance or cause allergies [22–24]. Researchers are working on other novel antimicrobial agents to deal with those antibiotic-resistant bacteria commonly encountered in clinical settings [25]. However, the development of new antimicrobial medications in clinical treatment cannot keep pace with the evolution of antibiotic resistance, thus creating a pressing need for innovative agents [26].

One widely accepted strategy is to discoveri novel compound structures. Nawrot et al. studied the synergistic effects of combining isoniazid and pyrazinamide with isoniazid and 4-aminosalicylic acid to enhance antibacterial activity (Fig. 1) [27]. Chen et al. synthesized innovative amide/sulfonamide derivatives and evaluated their inhibitory effects on IL-6 and TNF-α (Fig. 1) [28]. By studying the biosynthetic mechanism of lipopolysaccharides (LPS), a highly conserved LPS biosynthetic target MsbA protein was discovered. MsbA protein is one of the typical models for studying the ABC transporter superfamily. Its main function is to help transport lipopolysaccharides from the cytoplasmic side of the Gram negative bacterial endometrium to the periplasmic side of the endometrium [29]. Tetrahydrobenzothiophene derivatives have gained interest as potential antibacterial agents, including 2-(2-iodobenzamido)-6-methyl-4,5,6,7-tetrahydrobenzo[*b*]

* Corresponding authors.
E-mail addresses: peishuchen928@163.com (S. Pei), Wuwen_monica@outlook.com (W. Wu), guanshan87@163.com (S. Guan).

https://doi.org/10.1016/j.bioorg.2023.106932
Received 12 September 2023; Received in revised form 12 October 2023; Accepted 20 October 2023
Available online 21 October 2023

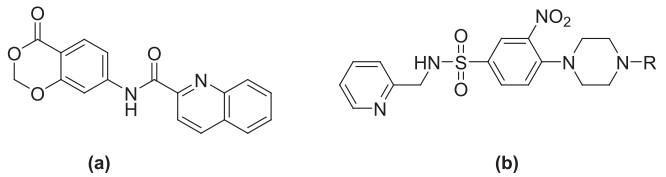

Fig. 1. (a) Design strategies for isoniazid and pyrazinamide with isoniazid and 4-aminosalicylic acid; (b) Design strategy for the target compounds of amide/sulfonamide derivatives.

thiophene-3-carboxylic acid (Fig. 2) [30,31], which exhibits significant bactericidal efficacy against *Escherichia coli*, *Staphyloco ccus aureus*, P*seudomonas aeruginosa*, and *Salmonella*. Using this structure as a lead compound for structural modification is a feasible strategy for obtaining new antibacterial agents.

In this study, we are now reporting a study for design and development of tetrahydrobenzothiophene derivatives against four types of bacteria, as shown in Fig. 2. The lead compound was modified by altering its 2-carboxyl group to amide or cyano groups. Sulfonamide structures, known for their antimicrobial efficacy, replaced the amide linkage in the primary compound to generate novel derivatives. Manipulating the carbon chain length in the cyclohexyl moiety was explored as a potential avenue for enhancing antibacterial activity. Functional groups like methoxy, fluorine atoms, and nitro groups were incorporated into the benzene ring to investigate their activity against both Gram-negative and Gram-positive bacteria and their toxicity to normal human liver cells. This study can provide useful information for the design of new analogues of tetrahydrobenzothiophene antibacterial with improved activity.

2. Results and discussion

2.1. Chemistry

The synthesis of novel tetrahydrobenzothiophene derivatives is demonstrated in Scheme 1 and Scheme 2. Cyclohexanone was employed as the initial substrate and underwent reaction with either acrylonitrile or cyanoacetamide in ethanol to yield two primary intermediates (**1a**-**1b**). These intermediates were subsequently reacted with benzoyl chloride derivatives or phenylacetyl chloride derivatives under basic catalysis in dichloromethane to obtain the desired compounds (**2a**-**2r**), as depicted in Scheme 1.

The influence of substituents in the starting materials led to the formation of various intermediate structures. These intermediates were then transformed into the final products through a three-step synthesis approach, as illustrated in Scheme 2. A series of cyclic ketones were subjected to a reaction with ethyl cyanoacetate and sulfur powder in the presence of ethanol as the solvent. By substituting the hydrogen atoms in the amino group with different benzoyl chloride derivatives or phenylacetyl chloride derivatives in the presence of a base, a series of intermediates (**4a**-**4 m** and **5a**-**5i**) were synthesized. These intermediates were subsequently hydrolyzed under basic conditions to yield the desired compounds (**6a**-**6v**). The structures of all synthesized compounds were thoroughly characterized using techniques such as proton nuclear magnetic resonance (^{1}H NMR), carbon-13 nuclear magnetic resonance (^{13}C NMR), and High Resolution Mass Spectrometer (HRMS). This comprehensive characterization ensures the accuracy of the proposed structures. Corresponding yield and melting point data are presented in the experimental section.

2.2. In vitro antibacterial activity assay

The evaluation of the inhibitory effect of tetrahydrobenzothiophene derivatives **2a**-**6v** on bacterial growth was conducted through a standard broth microdilution assay, as detailed in Table 1. Strains tested included *Escherichia coli* ATCC 25922, *Pseudomonas aeruginosa* ATCC 27853, *Salmonella* ATCC 12022, and *Staphylococcus aureus* ATCC 25922. Commercially available antibiotics, specifically ciprofloxacin and gentamicin, served as control substances in this study. In general, the majority of the newly synthesized tetrahydrobenzothiophene compounds listed in Table 1 and Table 2 demonstrated a range of inhibitory activity from moderate to good. Compounds **6n**, **6o**, **6p**, **6r**, and **6 s** exhibited significant antibacterial activity against *Escherichia coli*, *Pseudomonas aeruginosa*, *Salmonella*, and *Staphylococcus aureus*. Compound **6 s** demonstrated strong antibacterial activity against *Escherichia coli*, with a minimum inhibitory concentration (MIC) of 0.31 μM, and compound **6p** displayed a MIC of 0.31 μM against *Staphylococcus aureus*. The MIC values of several compounds were lower than that of ciprofloxacin and comparable to gentamicin, ranging from 0.20 to 2.20 μM. Compounds **2 g** and **2 h** exhibited good bactericidal activity against *Salmonella* and *Pseudomonas aeruginosa* with MIC values ranging from 0.91 to 1.19 μM. Compounds **2o**-**2p** exhibited significant antibacterial activity against *Salmonella* and *Pseudomonas aeruginosa* with MIC values ranging from 0.72 to 0.75 μM. Compounds **6c** and **6i** demonstrated good antibacterial efficacy against *Staphylococcus aureus*, *Salmonella*, and *Pseudomonas aeruginosa* with MIC values ranging from 0.56 to 2.45 μM. Compounds **6e** and **6 m** exhibited significant antibacterial activity against *Escherichia coli*, *Salmonella*, and *Pseudomonas aeruginosa* with MIC values ranging from 0.74 to 2.21 μM. The MIC values of eight compounds against *Staphylococcus aureus* ranged from 0.31 to 0.78 μM. Compounds **6n**, **6o**, **6p**, **6r**, and **6 s** demonstrated the highest level of antibacterial activity against *Staphylococcus aureus* and exhibited significant antibacterial activity against all tested bacteria when compared to other synthetic compounds and ciprofloxacin.

As indicated in Table 1 and Table 2, compound **6p** displayed good antibacterial activity and low cytotoxicity (SI = 1251.3), prompting further evaluation through an *in vitro* aging test. Time-kill curves of different concentrations of compound **6p** against *Staphylococcus aureus*, *Escherichia coli*, *Salmonella*, and *Pseudomonas aeruginosa* showed concentration-dependent bacteriostatic effects, as illustrated in Fig. 3. While the concentration of 0.5 × MIC exhibited higher antibacterial kinetics, the concentrations of 1 × and 2 × MIC demonstrated relative antibacterial kinetics. After treatment with derivatives, the bacterial viable cell count decreased to 1, 2 × MIC in almost 2 h.

2.3. Molecular docking

Tetrahydrobenzothiophene derivatives have been extensively documented for their binding affinity towards the MsbA target in bacteria.

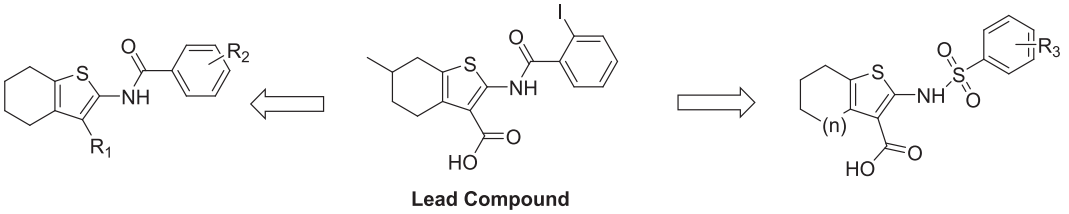

Fig. 2. Design of Tetrahydrobenzothiophene Derivatives.

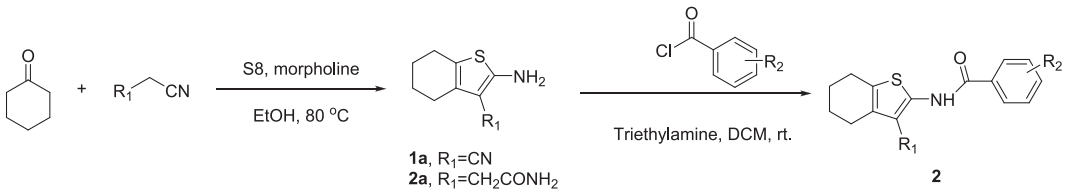

Scheme 1. The synthesis process of target compounds **2a-2r**.

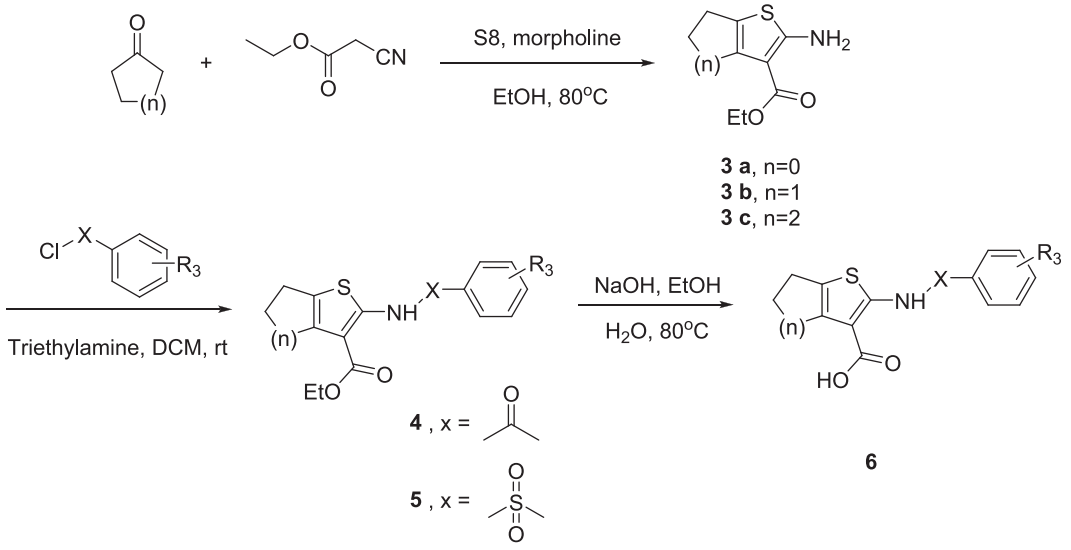

Scheme 2. The synthesis process of target compounds **6a-6v**.

This affinity interferes with the synthesis pathway of the bacterial outer membrane, leading to potent bactericidal effects [32]. Among the compounds studied, compound **6p** stands out due to its significant antibacterial activity, rendering it a key focus in this investigation. To assess the antibacterial efficacy of compound **6p**, computational simulations were performed to elucidate its potential binding affinity to the MsbA crystal structure of Salmonella typhimurium (PDB ID: 3B60). This binding may contribute partially to the antibacterial activity mechanism of this compound or offer insights for the development of more potent tetrahydrobenzothiophene derivatives. Molecular docking was conducted using a molecular operating environment to explore the potential interaction between **6p** and MsbA. The results show that the thiophene moiety plays a crucial role in the molecule's more stable conformation and fits closely with the active residue (Tyr −351). Notably, the interaction between acetic acid and asp-117 and tyr-393 was observed to occur partially through the formation of covalent bonds (Fig. 4). The multitude of binding modes has sparked our curiosity and motivated further investigation into this subject.

2.4. Wound healing studies in mice

The natural environment harbors a diverse range of bacteria, particularly in humid and warm conditions that provide optimal conditions for bacterial proliferation. Wounds create an optimal environment for bacterial proliferation. Building on this, we utilized a sterile mouse strain in our laboratory to establish a wound model for evaluating the wound antibacterial activity of tetrahydrobenzothiophene derivatives. Compound **6p**, which exhibited the highest activity in the *in vitro* antibacterial test (MIC = 0.31 μM), was selected as the subject of investigation for this study. After establishing the wound model in mice of experimental group, we used a microinjector to apply the drugs to the wound area. The control group was administered 20 μl of saline, while the experimental group received the test drug at a concentration of 250 μg/ml every other day. The wound area was measured on days 1, 3, 5, 7, and 9 (Fig. 5).

The structure of a drug can offer valuable insights into its specific functions. However, it's essential to recongnize that wound repair is an exceedingly intricate biological process in human life, involving a series of physiological and biochemical reactions during drug treatment. Therefore, conducting in vivo experiments is crucial for investigating the effectiveness of drugs. As depicted in Fig. 5, the wound area of the group treated with compound **6p** was notably smaller than that in the control group on the fifth day. By the seventh day, wounds in mice that received treatment with compound **6p** had nearly completely healed, whereas the control group still showed no apparent signs of healing by the ninth day. The findings presented in this study provide evidence of the involvement of compound **6p** in the wound healing process.

The MIC values varied between 0.31 and 0.49 μM. Structure-activity relationship (SAR) studies indicated that compounds within series 2, shown in Fig. 6, exhibited enhanced inhibitory effects when an electron-withdrawing group was present on the benzene ring and involving alterations to the functional groups of the thiophene ring and the structure of the benzene ring (compounds **2 g**, **2 h**, and **2r**). Excessive electron-withdrawing substituents on the benzene ring led to a decrease in antibacterial activity (e.g., compounds **2b** and **2 l**). When R_1 was cyano or formamide and R_2 was a substituted benzene ring, the compound exhibited a decrease in antibacterial activity. This decrease was observed in compounds **2a-2f** and **2i-2 l**. Conversely, when R_2 was a substituted methylbenzene group, the compound exhibited enhanced antibacterial activity, as evidenced by compounds **2 g**, **2 h**, and **2 m-2r**. The analysis of the SAR of compound series 6 involved modifications in the number of saturated alkanes in the lead compound and the linking groups between the benzene ring and thiophene ring. The results indicated that the antibacterial activity of the compounds increased when n = 0 and × was an amide group. Furthermore, the presence of electron-withdrawing groups on the benzene ring led to an enhancement in the

Table 1
Compounds were prepared, and the antibacterial activity was expressed as the minimum inhibitory concentration (MIC), and the cytotoxicity of human normal hepatocyte (L02) was expressed as half of the maximum inhibitory concentration (IC_{50}).

Code	Compound	Antimycobacterial Activity MIC [a] (μM)				IC_{50} (μM)	SI[c]
		Staphylococcus aureus	*Escherichia coli*	*Salmonella*	*Pseudomonas aeruginosa.*		
2a	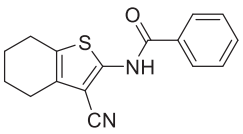	5.31	3.54	2.66	3.10	–	–
2b	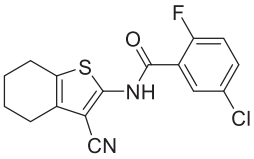	4.48	2.99	2.24	2.61	–	–
2c	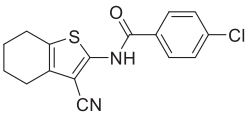	4.73	3.16	2.37	2.76	–	–
2d	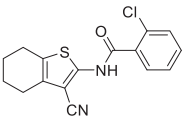	3.16	2.37	2.37	2.76	–	–
2e	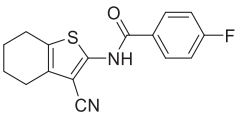	4.99	2.50	2.50	2.91	–	–
2f	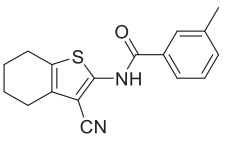	5.06	3.37	2.53	2.95	–	–
2 g	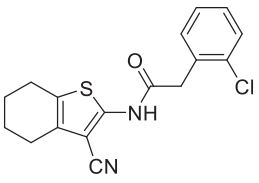	1.51	1.14	1.14	0.91	–	–
2 h	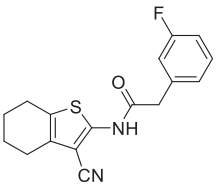	1.19	1.19	1.19	0.95	–	–

(*continued on next page*)

Table 1 (*continued*)

Code	Compound	Antimycobacterial Activity MIC [a] (μM)				IC_{50} (μM)	SI[c]
		Staphylococcus aureus	*Escherichia coli*	*Salmonella*	*Pseudomonas aeruginosa.*		
2i	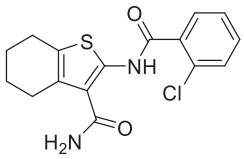	2.99	2.24	2.24	2.61	–	–
2j	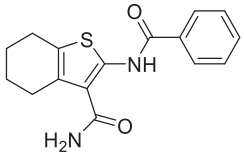	3.33	2.50	3.33	2.91	–	–
2 k	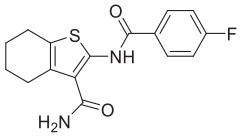	4.71	2.36	3.14	2.75	–	–
2 l	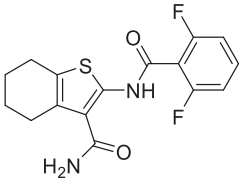	4.46	2.23	2.23	2.60	–	–
2 *m*	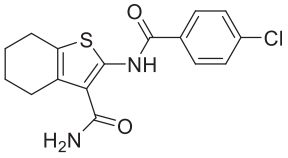	2.24	1.12	1.12	1.12	>150[b]	67.0
2*n*	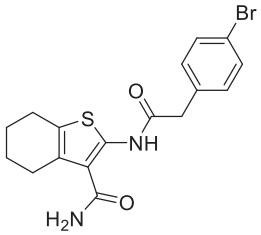	3.81	1.9	1.9	1.9	168.7 [b]	44.3

(*continued on next page*)

Table 1 (*continued*)

Code	Compound	Antimycobacterial Activity MIC [a] (μM)				IC_{50} (μM)	SI[c]
		Staphylococcus aureus	*Escherichia coli*	*Salmonella*	*Pseudomonas aeruginosa.*		
2o	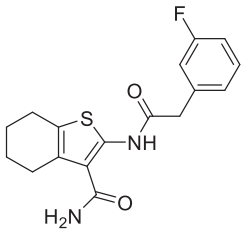	0.90	0.75	0.75	0.75	>150[b]	166.7
2p	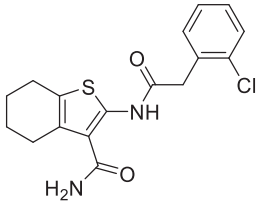	0.72	0.72	0.72	0.72	>150[b]	208.3
2q	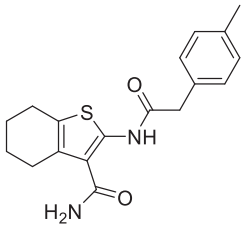	1.14	1.14	0.91	0.91	>150[b]	131.6
2r	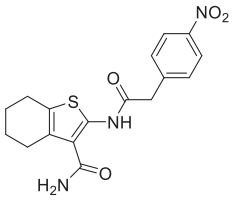	1.39	1.04	1.39	1.39	>150[b]	108.0
6a	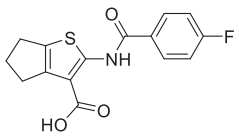	2.46	3.28	2.46	2.46	–	–
6b	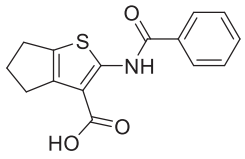	3.48	2.61	2.61	2.61	–	–

(*continued on next page*)

Table 1 (*continued*)

Code	Compound	Antimycobacterial Activity MIC [a] (μM)				IC_{50} (μM)	SI[c]
		Staphylococcus aureus	*Escherichia coli*	*Salmonella*	*Pseudomonas aeruginosa.*		
6c	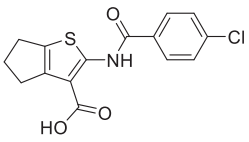	0.78	0.78	2.33	1.16	–	–
6d	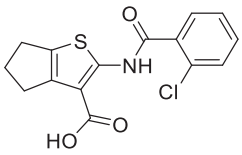	3.1	2.33	2.33	2.72	–	–
6e	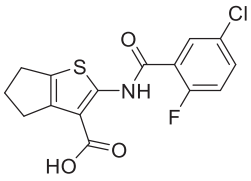	1.1	0.74	2.21	2.21	708.8	644.4
6f	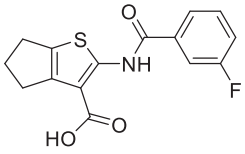	1.23	2.46	2.46	2.87	–	–
6 g	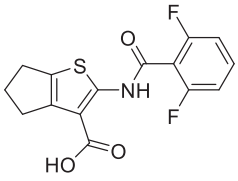	2.33	4.67	2.33	2.33	–	–
6 h	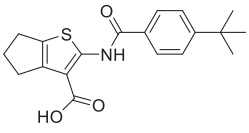	2.18	1.09	2.18	2.18	–	–
6i	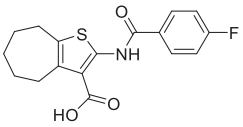	0.56	0.75	2.45	2.45	>150[b]	267.9

(*continued on next page*)

Table 1 (*continued*)

Code	Compound	Antimycobacterial Activity MIC [a] (μM)				IC_{50} (μM)	SI[c]
		Staphylococcus aureus	*Escherichia coli*	*Salmonella*	*Pseudomonas aeruginosa.*		
6j	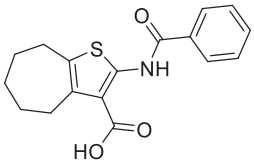	3.17	2.38	2.38	2.77	–	–
6 k	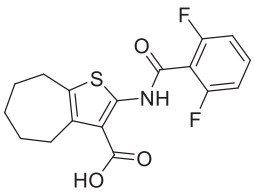	2.85	2.13	2.13	2.85	–	–
6 l	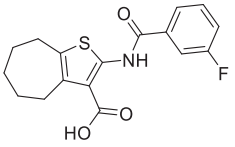	2.25	0.75	2.25	2.25	>150[b]	66.7
6 *m*	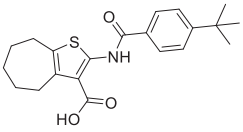	2.02	1.01	2.02	2.02	7.623[b]	3.8
Lead compound	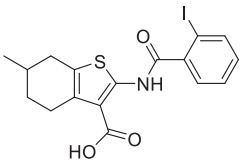	0.89	1.12	2.23	2.55	–	–
	Ciprofloxacin	1.13	1.13	1.51	2.26		
	Gentamicin	0.22	0.40	0.54	0.54		

"-" = not dissolved.

[a] The MIC values measured at pH = 7.0 (alkaline) are the test results at pH = 7.0 (neutral).

[b] Since the test compounds precipitated in the cell culture medium, higher concentrations could not be measured.

[c] Selectivity index (SI) = IC_{50} (μM)/MIC *Staphylococcus aureus* (μM) calculated for active compounds having MIC *Staphylococcus aureus* ≤ 250 μg/ml.

antibacterial activity, as demonstrated by compounds **6c** and **6e**. However, when n = 2, antibacterial activity decreased as the number of electron-withdrawing groups on the benzene ring increased (compounds **6i** and **6 k**). Compounds with a double-substituted electron-withdrawing group on the benzene ring exhibited comparable antibacterial activity to those with a potent electron-donating group (compounds 6 k and 6 m). Considering that sulfonamide functional groups have good bactericidal potential, SAR analysis revealed that tetrahydrobenzothiophene derivatives that only altered the structure of the lead compound's amide and benzene rings exhibited excellent antibacterial activity and good broad-spectrum bactericidal properties (compounds **6n**, **6o**, **6p**, **6r**, and **6 s**). Furthermore, when a compound's benzene ring was attached to a strong electron-withdrawing group, it exhibited enhanced antibacterial activity compared to a compound with an electron-donating group (compounds **6o** and **6p**). The antibacterial activity of halogen monosubstituted compounds on a benzene ring was comparable to that of potent substituents attached to a benzene ring, as demonstrated by compounds **6n** and **6o**.

3. Experiment section

3.1. Chemistry

3.1.1. General

All initial substances and chemicals utilized in this study are readily obtainable from commercial sources and can be employed without the

Table 2
Compounds were prepared, and the antibacterial activity was expressed as the minimum inhibitory concentration (MIC), and the cytotoxicity of human normal hepatocyte (L02) was expressed as half of the maximum inhibitory concentration (IC_{50}).

Code	Compound	Antimycobacterial Activity MIC[a] (μM)				IC_{50} (μM)	SI[c]
		Staphylococcus aureus	*Escherichia coli*	*Salmonella*	*, Pseudomonas aeruginosa.*		
6*n*	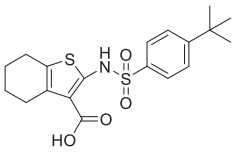	0.48	0.95	1.91	1.91	81.57[b]	170.0
6o	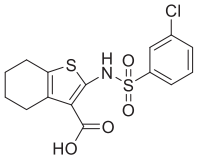	0.4	0.67	2.02	2.02	1.988	4.97
6p	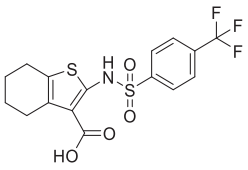	0.31	0.62	1.85	1.85	387.9 [b]	1251.3
6q	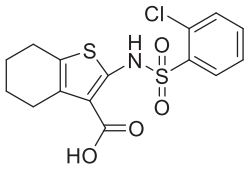	2.69	2.02	2.02	2.29	–	–
6r	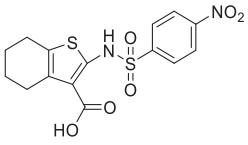	0.49	0.65	1.96	1.96	>150[b]	306.1
6 s	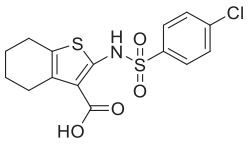	0.4	0.67	1.01	2.35	>150[b]	375
6 t	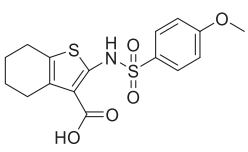	4.08	2.04	2.04	2.04	>150[b]	36.8

(*continued on next page*)

Table 2 (*continued*)

Code	Compound	Antimycobacterial Activity MIC[a] (μM)				IC_{50} (μM)	SI[c]
		Staphylococcus aureus	*Escherichia coli*	*Salmonella*	, *Pseudomonas aeruginosa*.		
6u	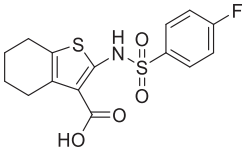	4.22	2.11	2.11	2.11	–	–
6v	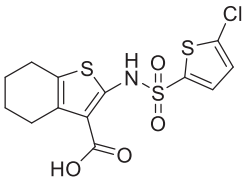	0.99	0.99	1.98	1.98	–	–
Lead compound	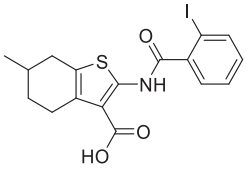	0.89	1.12	2.23	2.55	–	–
	Ciprofloxacin	1.13	1.13	1.51	2.26	–	–
	Gentamicin	0.22	0.40	0.54	0.54	–	–

"-" = not dissolved.

[a] The MIC values measured at pH = 7.0 (alkaline) are the test results at pH = 7.0 (neutral).

[b] Since the test compounds precipitated in the cell culture medium, higher concentrations could not be measured.

[c] Selectivity index (SI) = IC_{50} (μM)/MIC *Staphylococcus aureus* (μM) calculated for active compounds having MIC *Staphylococcus aureus* ≤ 250 μg/ml.

need for additional purification. TLC analysis was conducted utilizing Merck silica gel DF 254 plates. 1H and 13C nuclear magnetic resonance (NMR) spectra were acquired using a Varian Inova400 (^{1}H at 400 MHz and ^{13}C at 101 MHz) using $CDCl_3$ or DMSO-d_6 as solvents. Chemical shifts are commonly denoted in δ (ppm), whereas coupling constants (J) are typically expressed in Hz. High-resolution mass (HRMS) spectra were acquired using a Bruker Maxis Impact Q-TOF instrument (Bruker, Billerica, USA) and a Dionex Ultimate 3000 spectrometer (Dionex, Sunnyvale, USA).

3.1.2. General procedure for the synthesis of compound intermediates ***1a***

To a solution of cyclohexanone (0.1 mol) in anhydrous ethanol and acrylonitrile (0.12 mol), morpholine (0.15 mol), and sulfur (0.12 mol) were added. The reaction mixture was stirring at 80 °C for 2 h. After confirming the completion of the reaction by TLC, the reaction mixture was concentrated and extracted with ethyl acetate. The organic layer was combined, washed with brine and dried over Na_2SO_4. Evaporation of the solvent afforded products **1a** without any purification.

3.1.3. General procedure for the synthesis of compound intermediates ***2a***

To a solution of cyclohexanone (0.1 mol) in anhydrous ethanol, cyanacetylurea (0.12 mol), morpholine (0.15 mol), and sulfur (0.12 mol) were added. The reaction mixture was stirred at 80 °C for 2 h. After confirming the completion of the reaction by TLC, the reaction mixture was concentrated and extracted with ethyl acetate. The organic layer was combined, washed with brine and dried over Na_2SO_4. Evaporation of the solvent afforded products **2a** without any purification.

3.1.4. General procedure for the synthesis of compounds ***2a-2r***

To a solution of compounds **1a-1b** (1 g, 5.61 mmol) in dichloromethane, triethylamine (0.851 g, 8.42 mmol) was added. The mixture was stirred at a temperature of 0 °C. Benzoyl chloride derivatives or phenylacetyl chloride derivatives (8.42 mmol) was added and stirred at 25 ℃ overnight. After confirming the completion of the reaction by TLC, the reaction mixture was quenched by adding water and extracted with DCM. The organic layer was combined, washed with brine and dried over Na_2SO_4. Evaporation of the solvent afforded a mixture of expected products. The mixture was purified using silica gel column chromatography (hexane/ethyl acetate = 10/1) to obtain the desired products **2a-2r**.

3.1.5. General procedure for the synthesis of compound intermediates ***3a-3c***

To a solution of cyclopentanone (cyclohexanone or cycloheptanone) (0.1 mol) in 100 ml ethanol, ethyl cyanoacetate (0.12 mol), morpholine (0.15 mol), and sulfur (0.12 mol) were added. The mixture was stirred at a temperature of 80 °C for 2 h. After confirming the completion of the reaction by TLC, the reaction mixture was concentrated and extracted with ethyl acetate. The organic layer was combined, washed with brine and dried over Na_2SO_4. The mixture was purified using silica gel column chromatography (hexane/ethyl acetate = 20/1) to obtain the desired products **3a-3c.**

3.1.6. General procedure for the synthesis of compound intermediates ***4a-4m***

To a solution of compounds **3a-3c** (1 g, 4.74 mmol) in

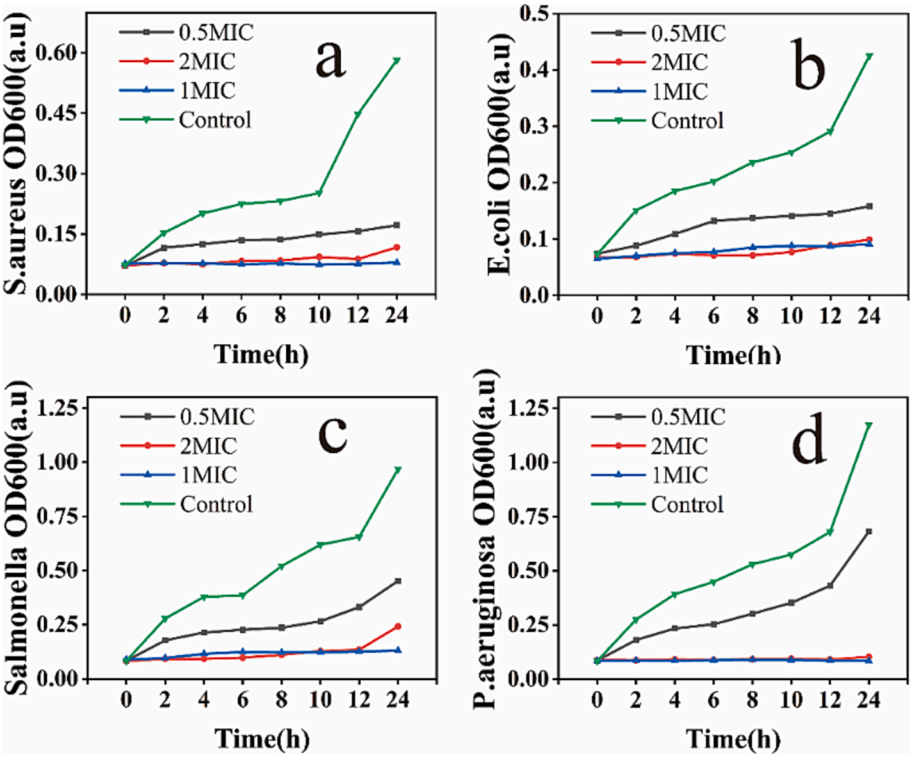

Fig. 3. Analysis of killing time of compound **6p** against *Staphylococcus aureus*, *Escherichia coli*, *Salmonella* and *Pseudomonas aeruginosa*.

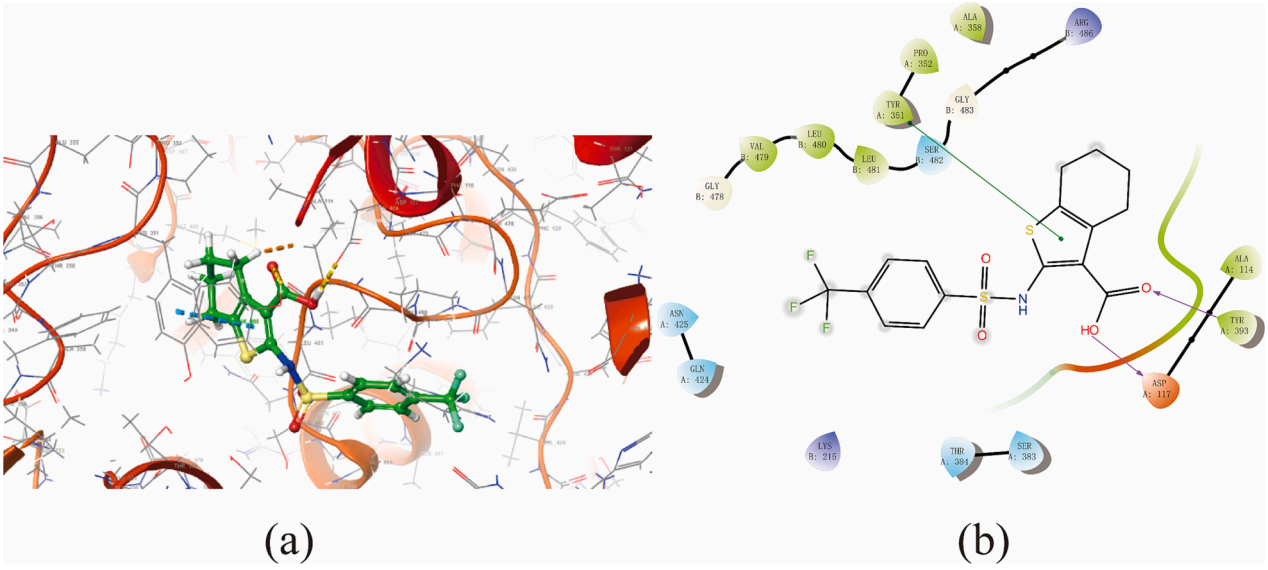

Fig. 4. The best docking results of compound 3B with the crystal structure of Salmonella typhimurium (PDB ID: 3B60) MsbA. (a) 3D docking model;(b) plane docking model.

dichloromethane, triethylamine (0.72 g, 7.11 mmol) was added. The mixture was stirred at a temperature of 0 °C. Phenylacetyl chloride derivatives (7.11 mmol) was added and stirred at 25 ℃ overnight. After confirming the completion of the reaction by TLC, the reaction mixture was quenched by adding water and extracted with DCM. The organic layer was combined, washed with brine and dried over Na_2SO_4. Evaporation of the solvent afforded a mixture of expected products. The mixture was purified using silica gel column chromatography (hexane/ethyl acetate = 20/1) to obtain the desired products **4a-4 m**.

*3.1.7. General procedure for the synthesis of compound intermediates **5a-5i***

To a solution of compounds **3b** (1 g, 4.74 mmol) in dichloromethane, triethylamine (0.72 g, 7.11 mmol) was added. The mixture was stirred at a temperature of 0 °C. Phenylacetyl chloride derivatives (7.11 mmol) was added and stirred at 25 ℃ overnight. After confirming the completion of the reaction by TLC, the reaction mixture was quenched by adding water and extracted with DCM. The organic layer was combined, washed with brine and dried over Na_2SO_4. Evaporation of the solvent afforded a mixture of expected products. The mixture was purified using silica gel column chromatography (hexane/ethyl acetate =

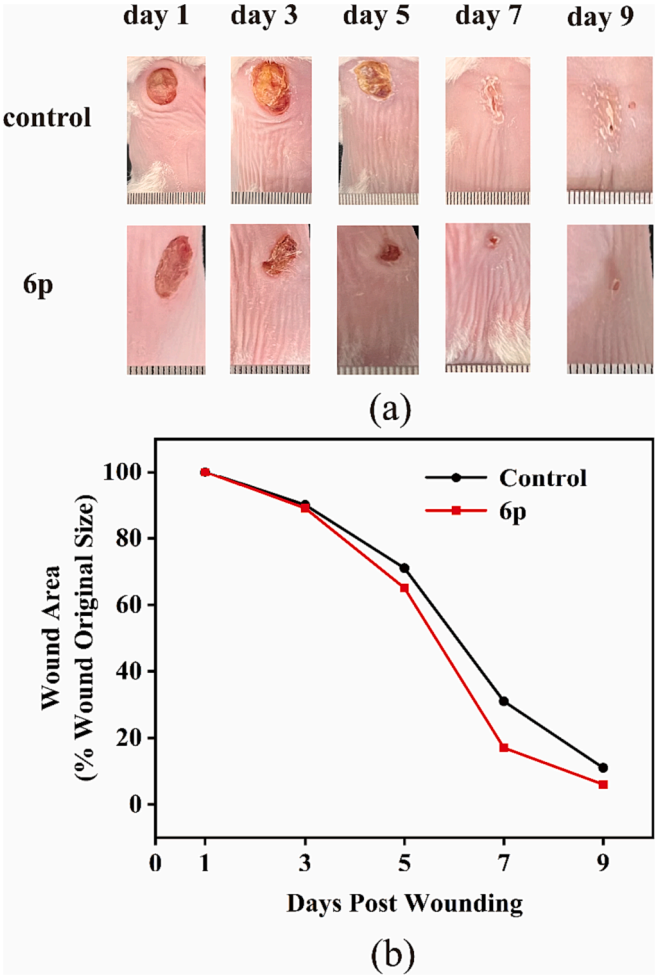

Fig. 5. (a)Time diagram of wound healing in mice;(b) Mice wound area.

20/1) to obtain the desired products **5a-5i.**

*3.1.8. General procedure for the synthesis of compounds **6a-6v***

To a solution of compounds **4a-4 m** and **5a-5i** (1 g) in ethanol, and 20 ml of 1 M NaOH was added. The mixture was stirred at 80 °C for 2 h. After confirming the completion of the reaction by TLC, 1 M HCl was added, and adjust the pH to a range of 2 to 3. The reaction mixture adding water and extracted with ethyl acetate. The organic layer was combined, washed with brine and dried over Na_2SO_4. Evaporation of the solvent afforded a mixture of expected products. The mixture was purified using silica gel column chromatography (hexane/ethyl acetate = 110/1) to obtain the desired product **6a-6v**.

3.2. Analytical data

*3.2.1. N-(3-cyano-4,5,6,7-tetrahydrobenzo[b]thiophen-2-yl)benzamide **(2a)***

White solid; Yield 60 %; M.p. 195.4–196.4 °C. ^{1}H NMR (400 MHz, DMSO-d_6) δ 12.31 (s, 1H), 8.08 – 7.17 (m, 5H), 2.65 (d, J = 5.0 Hz, 4H), 1.78 (s, 4H). ^{13}C NMR (101 MHz, DMSO) δ 164.93, 146.14, 135.17, 132.20, 131.77, 130.72, 130.02, 129.89, 128.65, 127.63, 114.43, 94.95, 24.04, 23.89, 23.07, 22.18. HRMS (ESI): calcd for: $C_{16}H_{14}N_2OS$, *m/z* $[M + H]^+$ 282.0827, found 282.0825.

*3.2.2. 5-chloro-N-(3-cyano-4,5,6,7-tetrahydrobenzo[b]thiophen-2-yl)-2-fluorobenzamide**(2b)***

White solid; Yield 58.1 %; M.p. 199.6–200.6 °C. ^{1}H NMR (400 MHz, DMSO-d_6) δ 12.10 (s, 1H), 8.04 – 7.18 (m, 3H), 2.59 (dd, J = 41.7, 5.7 Hz, 4H), 1.78 (s, 4H). ^{13}C NMR (101 MHz, DMSO) δ 161.21, 159.69, 157.20(d, J = 9.1 Hz, 1F), 145.98, 133.55, 131.80, 130.29, 128.89, 124.56, 118.86, 114.41, 95.33, 24.02, 23.88, 23.04, 22.15. HRMS (ESI): calcd for: $C_{16}H_{12}ClFN_2OS$, *m/z* $[M + H]^+$ 334.0343, found 334.0347.

*3.2.3. 4-chloro-N-(3-cyano-4,5,6,7-tetrahydrobenzo[b]thiophen-2-yl) benzamide**(2c)***

White solid; Yield 59.2 %; M.p. 179.6–180.6 °C. ^{1}H NMR (400 MHz, DMSO-d_6) δ 11.79 (s, 1H), 8.30 – 6.93 (m, 4H), 2.59 (dt, J = 38.0, 5.1 Hz, 4H), 1.78 (q, J = 4.9, 4.0 Hz, 4H). ^{13}C NMR (101 MHz, DMSO) δ 164.63, 146.50, 137.81, 131.92, 131.61, 130.72, 129.25, 129.03, 114.62, 96.54, 24.08, 23.93, 23.06, 22.17. HRMS (ESI): calcd for: $C_{16}H_{13}ClN_2OS$, *m/z* $[M + H]^+$ 316.0437, found 316.0432.

*3.2.4. 2-chloro-N-(3-cyano-4,5,6,7-tetrahydrobenzo[b]thiophen-2-yl) benzamide**(2d)***

White solid; Yield 56.3 %; M.p. 196.5–197.5 °C. ^{1}H NMR (400 MHz, DMSO-d_6) δ 12.31 (s, 1H), 7.98 – 7.08 (m, 4H), 2.65 (d, J = 5.0 Hz, 4H), 1.78 (s, 4H). ^{13}C NMR (101 MHz, DMSO) δ 164.91, 146.14, 135.19, 132.18, 131.75, 130.74, 130.02, 129.89, 128.64, 127.61, 114.43, 94.97,

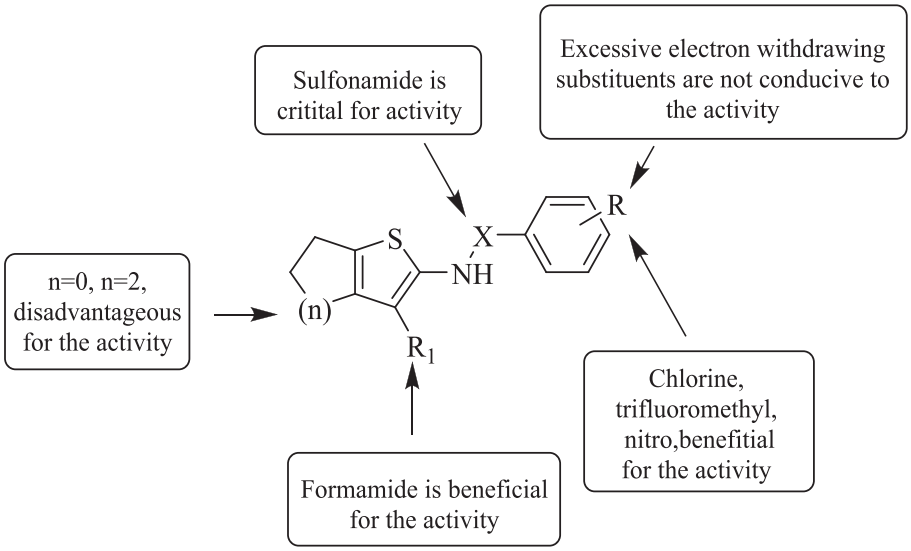

Fig. 6. Structure-Activity Relationship of Tetrahydrobenzothiophene derivatives.

24.05, 23.89, 23.08, 22.19. HRMS (ESI): calcd for: $C_{16}H_{13}ClN_2OS$, *m/z* $[M + H]^+$ 316.0437, found 316.0431.

3.2.5. N-(3-cyano-4,5,6,7-tetrahydrobenzo[b]thiophen-2-yl)-4-fluorobenzamide(2e)

White solid; Yield 59.3 %; M.p. 198.2–199.2 °C. ^{1}H NMR (400 MHz, DMSO-d_6) δ 11.73 (s, 1H), 8.24 – 7.25 (m, 4H), 2.63 (d, J = 4.9 Hz, 4H), 2.00 – 1.51 (m, 4H). ^{13}C NMR (101 MHz, DMSO) δ 166.28(d, J = 2.3 Hz, 1F), 164.56, 163.79, 146.66, 131.85, 131.68, 131.59, 129.38, 129.12, 116.06, 115.84, 114.64, 96.41, 24.08, 23.07, 22.18. HRMS (ESI): calcd for: $C_{16}H_{13}FN_2OS$, *m/z* $[M + H]^+$ 300.0733, found 300.0735.

3.2.6. N-(3-cyano-4,5,6,7-tetrahydrobenzo[b]thiophen-2-yl)-3-methylbenzamide(2f)

White solid; Yield 61.3 %; M.p. 197.3–198.3 °C. ^{1}H NMR (400 MHz, DMSO-d_6) δ 11.98 (s, 1H), 8.00 – 6.84 (m, 4H), 2.59 (dd, J = 43.3, 5.4 Hz, 4H), 2.38 (s, 3H), 1.95 – 1.62 (m, 14). ^{13}C NMR (101 MHz, DMSO) δ 167.65, 146.58, 136.34, 135.10, 131.66, 131.01, 130.84, 128.52, 128.30, 126.03, 114.55, 95.29, 24.07, 23.91, 23.11, 22.22, 19.87. HRMS (ESI): calcd for: $C_{17}H_{16}N_2OS$, *m/z* $[M + H]^+$ 296.0983, found 296.0984.

3.2.7. 2-(2-chlorophenyl)-N-(3-cyano-4,5,6,7-tetrahydrobenzo[b]thiophen-2-yl)aceta-mide(2 g)

Brown solid; Yield 59.1 %; M.p. 175.2–176.2 °C. ^{1}H NMR (400 MHz, DMSO-d_6) δ 11.85 (s, 1H), 8.30 – 7.04 (m, 4H), 4.04 (s, 2H), 2.65 – 2.29 (m, 4H), 1.92 – 1.55 (m, 4H). ^{13}C NMR (101 MHz, DMSO) δ 168.41, 147.00, 134.15, 133.74, 132.65, 131.20, 129.52, 129.29, 127.65, 127.60, 114.73, 93.04, 23.98, 23.77, 23.07, 22.18. HRMS (ESI): calcd for: $C_{17}H_{15}ClN_2OS$, *m/z* $[M + H]^+$ 330.0594, found 330.0599.

3.2.8. N-(3-cyano-4,5,6,7-tetrahydrobenzo[b]thiophen-2-yl)-2-(3-fluorophenyl)aceta-mide(2 h)

Brown solid; Yield 57.6 %; M.p. 177.1–178.1 °C. ^{1}H NMR (400 MHz, DMSO-d_6) δ 11.77 (s, 1H), 7.48 – 6.83 (m, 4H), 3.89 (s, 2H), 2.65 – 2.27 (m, 4H), 1.88 – 1.66 (m, 4H). ^{13}C NMR (101 MHz, DMSO) δ 168.91(d, J = 8.4 Hz, 1F), 146.86, 131.21, 130.70, 127.79, 125.92, 116.68, 116.47, 114.71, 114.15, 113.94, 93.23, 23.96, 23.76, 23.05, 22.16. HRMS (ESI): calcd fo: $C_{17}H_{15}FN_2OS$, *m/z* $[M + H]^+$ 314.0889, found 314.0892.

3.2.9. 2-(2-chlorobenzamido)-4,5,6,7-tetrahydrobenzo[b]thiophene-3-carboxamide(2i)

Yellow solid; Yield 59.3 %; M.p. 245.6–246.6 °C ; ^{1}H NMR (500 MHz, DMSO-d_6) δ 12.34 (s, 2H), 7.96 – 7.31 (m, 4H), 2.70 (dt, J = 31.6, 6.0 Hz, 4H), 1.75 (q, J = 6.7 Hz, 4H). ^{13}C NMR (126 MHz, DMSO) δ 167.74, 162.68, 141.99, 134.43, 132.86, 130.82, 130.58, 130.26, 129.75, 128.18, 127.32, 117.75, 25.60, 24.33, 22.95, 22.82. HRMS (ESI): calcd for: $C_{16}H_{15}ClN_2O_2S$, *m/z* $[M + H]^+$ 334.0543, found 334.0548.

3.2.10. 2-benzamido-4,5,6,7-tetrahydrobenzo[b]thiophene-3-carboxamide(2j)

White solid; Yield 59.5 %; M.p. 249.8–250.8 °C. ^{1}H NMR (500 MHz, DMSO-d_6) δ 13.08 (s, 2H), 8.05 – 7.47 (m, 5H), 2.84 – 2.59 (m, 4H), 1.76 (s, 4H). ^{13}C NMR (126 MHz, DMSO) δ 168.38, 162.75, 143.87, 133.01, 132.84, 129.62, 129.59, 127.42, 126.89, 116.36, 25.71, 24.36, 22.92, 22.83. HRMS (ESI): calcd for: $C_{16}H_{16}N_2O_2S$, *m/z* $[M + H]^+$ 300.0932, found 300.0938.

3.2.11. 2-(4-fluorobenzamido)-4,5,6,7-tetrahydrobenzo[b]thiophene-3-carboxamide(2 k)

White solid; Yield 58.8 %; M.p. 241.2–242.2 °C. ^{1}H NMR (500 MHz, DMSO-d_6) δ 13.04 (s, 2H), 7.70 (d, J = 252.3 Hz, 4H), 2.71 (d, J = 46.7 Hz, 4H), 1.76 (s, 4H). ^{13}C NMR (126 MHz, DMSO) δ 168.33, 165.99(d, J = 2.8 Hz, 1F), 164.00, 161.80, 143.69, 130.27, 129.64, 129.45, 25.68, 24.35, 22.91, 22.81. HRMS (ESI): calcd for: $C_{16}H_{15}FN_2O_2S$, *m/z* $[M + H]^+$ 318.0838, found 318.0833.

3.2.12. 2-(2,6-difluorobenzamido)-4,5,6,7-tetrahydrobenzo[b]thiophene-3-carboxamide(2 l)

Yellow solid; Yield 61.3 %; M.p. 246.3–247.3 °C. ^{1}H NMR (500 MHz, DMSO-d_6) δ 12.32 (s, 2H), 7.47 (dt, J = 186.6, 7.7 Hz, 3H), 2.69 (dt, J = 21.6, 6.0 Hz, 4H), 1.76 (p, J = 7.6, 6.4 Hz, 4H). ^{13}C NMR (126 MHz, DMSO) δ 167.50, 160.70(m, J = 9.9 Hz, 2F), 158.75, 156.54, 140.65, 133.89, 129.88, 127.58, 118.66, 113.08, 25.48, 24.30, 22.95, 22.78. HRMS (ESI): calcd for: $C_{16}H_{14}F_2N_2O_2S$, *m/z* $[M + H]^+$ 336.0744, found 336.0747.

3.2.13. 2-(4-chlorobenzamido)-4,5,6,7-tetrahydrobenzo[b]thiophene-3-carboxamide(2 m)

Yellow solid; Yield 63.7 %; M.p. 245.3–246.3 °C. ^{1}H NMR (500 MHz, DMSO-d_6) δ 13.08 (s, 2H), 8.08 – 7.38 (m, 4H), 2.87 – 2.61 (m, 4H), 1.75 (s, 4H). ^{13}C NMR (126 MHz, DMSO) δ 168.30, 161.77, 143.55, 137.80, 129.71, 129.34, 127.11, 116.66, 25.67, 24.36, 22.90, 22.80. HRMS (ESI): calcd for: $C_{16}H_{15}ClN_2O_2S$, *m/z* $[M + H]^+$ 334.0543, found 334.0549.

3.2.14. 2-(2-(4-bromophenyl)acetamido)-4,5,6,7-tetrahydrobenzo[b]thiophene-3-carboxamide(2n)

Yellow solid; Yield 58.2 %; M.p. 223.7–224.7 °C. ^{1}H NMR (500 MHz, DMSO- d_6) δ 11.58 (s, 2H), 7.42 (dd, J = 120.8, 8.0 Hz, 4H), 3.80 (s, 2H), 2.77 – 2.59 (m, 4H), 1.70 (p, J = 6.6, 6.0 Hz, 4H). ^{13}C NMR (126 MHz, DMSO) δ 167.70, 167.59, 142.15, 134.63, 132.24, 131.88, 129.35, 126.45, 120.69, 116.99, 42.15, 25.53, 24.23, 22.95, 22.84. HRMS (ESI): calcd for: $C_{17}H_{17}BrN_2O_2S$, *m/z* $[M + H]^+$ 392.0194, found 393.0190.

3.2.15. 2-(2-(3-fluorophenyl)acetamido)-4,5,6,7-tetrahydrobenzo[b]thiophene-3-carboxamide(2o)

Yellow solid; Yield 52.5 %; M.p. 176.5–177.5 °C. ^{1}H NMR (400 MHz, DMSO- d_6) δ 11.59 (s, 1H), 7.66 – 6.88 (m, 4H), 3.85 (s, 2H), 2.62 (dt, J = 28.3, 6.0 Hz, 4H), 1.72 (p, J = 6.6 Hz, 4H). ^{13}C NMR (101 MHz, DMSO) δ 167.60, 163.84(d, J = 8.6 Hz, 1F), 161.42, 142.17, 137.78, 130.84, 129.34, 126.45, 126.19, 116.99, 116.94, 116.73, 114.41, 114.20, 25.54, 24.22, 22.95. HRMS (ESI): calcd for: $C_{17}H_{17}FN_2O_2S$, *m/z* $[M + H]^+$ 332.0995, found 332.0992.

3.2.16. 2-(2-(2-chlorophenyl)acetamido)-4,5,6,7-tetrahydrobenzo[b]thiophene-3-carboxamide(2p)

Yellow solid; Yield 55.7 %; M.p. 177.9–178.9 °C. ^{1}H NMR (400 MHz, DMSO- d_6) δ 11.67 (s, 1H), 7.42 (dtd, J = 51.0, 5.6, 2.6 Hz, 4H), 3.93 (d, J = 1.8 Hz, 2H), 2.63 (dd, J = 27.2, 5.5 Hz, 4H), 1.72 (p, J = 6.4, 6.0 Hz, 4H). ^{13}C NMR (101 MHz, DMSO) δ 167.68, 166.83, 142.56, 134.28, 133.01, 132.87, 129.81, 129.75, 129.30, 127.97, 126.39, 116.60, 25.57, 24.24, 22.93, 22.84. HRMS (ESI): calcd for: $C_{17}H_{17}ClN_2O_2S$, *m/z* $[M + H]^+$ 348.0699, found 348.0695.

3.2.17. 2-(2-(p-tolyl)acetamido)-4,5,6,7-tetrahydrobenzo[b]thiophene-3-carboxamide(2q)

Green solid; Yield 56.2 %; M.p. 172.3–173.3 °C. ^{1}H NMR (400 MHz, DMSO-d_6) δ 11.58 (s, 1H), 7.50 – 6.57 (m, 4H), 3.73 (s, 2H), 2.63 (dd, J = 26.9, 5.5 Hz, 4H), 2.29 (s, 3H), 1.72 (t, J = 5.8 Hz, 4H). ^{13}C NMR (101 MHz, DMSO) δ 168.28, 167.62, 142.44, 136.45, 132.06, 129.72, 129.64, 129.28, 126.30, 116.70, 25.54, 24.22, 22.95, 22.85, 21.17. HRMS (ESI): calcd for: $C_{18}H_{20}N_2O_2S$, *m/z* $[M + H]^+$ 328.1245, found 328.1248.

3.2.18. 2-(2-(4-nitrophenyl)acetamido)-4,5,6,7-tetrahydrobenzo[b]thiophene-3-carboxamide(2r)

Brown solid; Yield 58.3 %; M.p. 177.9–178 °C. ^{1}H NMR (400 MHz, DMSO-d_6) δ 11.59 (s, 1H), 8.43 – 7.31 (m, 4H), 4.02 (s, 2H), 2.74 – 2.55 (m, 4H), 1.83 – 1.64 (m, 4H). ^{13}C NMR (101 MHz, DMSO) δ 167.51, 167.05, 147.03, 143.35, 141.72, 131.43, 129.45, 126.60, 124.00, 117.40, 25.49, 24.22, 22.95, 22.82. HRMS (ESI): calcd for:

$C_{17}H_{17}N_3O_4S$, *m/z* $[M + H]^+$ 359.0940, found 359.0945.

3.2.19. 2-(4-fluorobenzamido)-5,6-dihydro-4H-cyclopenta[b]thiophene-3-carboxylic acid(6a)

White solid; Yield 63.4 %; M.p. 231.5–232.5 °C. ^{1}H NMR (400 MHz, DMSO-d_6) δ 13.16 (s, 1H), 12.04 (s, 1H), 8.12 – 6.96 (m, 4H), 2.81 (q, J = 8.0 Hz, 4H), 2.31 (p, J = 7.3 Hz, 2H). ^{13}C NMR (101 MHz, DMSO) δ 167.61, 166.35(d, J = 2.3 Hz, 1F), 163.85, 161.80, 151.02, 142.03, 132.05, 130.29, 129.01, 116.82, 109.76, 30.19, 28.81, 27.85. HRMS (ESI): calcd for: $C_{15}H_{12}FNO_3S$, *m/z* $[M + H]^+$ 305.0522, found 305.0527.

3.2.20. 2-benzamido-5,6-dihydro-4H-cyclopenta[b]thiophene-3-carboxylic acid(6b)

White solid; Yield 53.5 %; M.p. 234.2–235.2 °C. ^{1}H NMR (400 MHz, DMSO- d_6) δ 13.20 (s, 1H), 12.10 (s, 1H), 8.22 – 7.31 (m, 5H), 2.83 (q, J = 8.2 Hz, 4H), 2.33 (p, J = 7.3 Hz, 2H). ^{13}C NMR (101 MHz, DMSO) δ 167.65, 162.87, 151.12, 142.07, 133.23, 132.44, 132.06, 129.70, 127.46, 109.72, 30.22, 28.85, 27.90. HRMS (ESI): calcd for: $C_{15}H_{13}NO_3S$, *m/z* $[M + H]^+$ 287.0616, found 287.0612.

3.2.21. 2-(4-chlorobenzamido)-5,6-dihydro-4H-cyclopenta[b]thiophene-3-carboxylic acid(6c)

White solid; Yield 60.5 %; M.p. 241.9–242.9 °C. ^{1}H NMR (400 MHz, DMSO- d_6) δ 13.22 (s, 1H), 12.09 (s, 1H), 8.08 – 7.13 (m, 4H), 2.83 (q, J = 7.8 Hz, 4H), 2.33 (p, J = 7.3 Hz, 2H). ^{13}C NMR (101 MHz, DMSO) δ 167.60, 161.92, 150.84, 142.13, 138.07, 132.27, 131.25, 129.79, 129.38, 109.98, 30.21, 28.86, 27.89. HRMS (ESI): calcd for: $C_{15}H_{12}ClNO_3S$, *m/z* $[M + H]^+$ 321.0226, found 321.0228.

3.2.22. 2-(2-chlorobenzamido)-5,6-dihydro-4H-cyclopenta[b]thiophene-3-carboxylic acid(6d)

White solid; Yield 60.5 %; M.p. 236.1–237.1 °C. ^{1}H NMR (400 MHz, DMSO- d_6) δ 13.20 (s, 1H), 11.71 (s, 1H), 7.97 – 7.33 (m, 4H), 2.84 (q, J = 6.4 Hz, 4H), 2.33 (p, J = 7.3 Hz, 2H). ^{13}C NMR (101 MHz, DMSO) δ 167.10, 162.54, 149.88, 142.24, 133.61, 133.27, 132.48, 130.99, 130.67, 130.57, 128.33, 110.32, 30.24, 28.87, 27.94. HRMS (ESI): calcd for: $C_{15}H_{12}ClNO_3S$, *m/z* $[M + H]^+$ 321.0226, found 321.0229.

3.2.23. 2-(5-chloro-2-fluorobenzamido)-5,6-dihydro-4H-cyclopenta[b]thiophene-3-carboxylic acid(6e)

White solid; Yield 53.8 %; M.p. 237.6–238.6 °C. ^{1}H NMR (400 MHz, DMSO- d_6) δ 13.17 (s, 1H), 12.20 (s, 1H), 8.04 – 7.17 (m, 3H), 2.83 (q, J = 7.4 Hz, 4H), 2.32 (p, J = 7.4 Hz, 2H). ^{13}C NMR (101 MHz, DMSO) δ 166.90, 158.04, 157.78(d, J = 8.5 Hz, 1F), 149.69, 142.35, 134.92, 132.98, 131.17, 129.77, 121.29, 119.28, 110.54, 30.26, 28.86, 27.89. HRMS (ESI): calcd for: $C_{15}H_{11}ClFNO_3S$, *m/z* $[M + H]^+$ 339.0132, found 339.0131.

3.2.24. 2-(3-fluorobenzamido)-5,6-dihydro-4H-cyclopenta[b]thiophene-3-carboxylic acid(6f)

Green solid; yield 54.1 %; M.p. 229.5–230.5 °C. ^{1}H NMR (400 MHz, DMSO-d_6) δ 13.18 (s, 1H), 12.06 (s, 1H), 7.93 – 7.10 (m, 4H), 2.80 (q, J = 7.8 Hz, 4H), 2.30 (p, J = 7.3 Hz, 2H). ^{13}C NMR (101 MHz, DMSO) δ 167.55, 163.92(d, J = 6.7 Hz, 1F), 161.47, 150.68, 142.10, 134.89, 132.25, 131.91, 123.29, 120.15, 114.62, 110.02, 30.15, 28.79, 27.84. HRMS (ESI): calcd for: $C_{15}H_{12}FNO_3S$, *m/z* $[M + H]^+$ 305.0522, found 305.0527.

3.2.25. 2-(2,6-difluorobenzamido)-5,6-dihydro-4H-cyclopenta[b]thiophene-3-carboxylic acid(6 g)

White solid; Yield 63.1 %; M.p. 231.7–232.7 °C. ^{1}H NMR (400 MHz, DMSO-d_6) δ 13.17 (s, 1H), 11.72 (s, 1H), 7.87 – 7.04 (m, 3H), 2.84 (q, J = 6.6 Hz, 4H), 2.34 (q, J = 7.2 Hz, 2H). ^{13}C NMR (101 MHz, DMSO) δ 166.86, 161.27, 158.77(m, J = 9.6 Hz, 2F), 156.55, 149.18, 142.33, 134.37, 132.70, 113.29, 113.03, 112.47, 110.63, 30.24, 28.86, 27.91. HRMS (ESI): calcd for: $C_{15}H_{11}F_2NO_3S$, *m/z* $[M + H]^+$ 323.0428, found 323.0422.

3.2.26. 2-(4-(tert-butyl)benzamido)-5,6-dihydro-4H-cyclopenta[b]thiophene-3-carboxylic acid(6 h)

White solid; Yield 59.1 %; M.p. 238.6–239.6 °C. ^{1}H NMR (400 MHz, DMSO-d_6) δ 13.25 – 12.91 (s, 1H), 12.06 (s, 1H), 7.73 (ddd, J = 86.7, 8.4, 1.8 Hz, 3H), 2.82 (dt, J = 13.7, 7.1 Hz, 4H), 2.32 (q, J = 7.2 Hz, 2H), 1.31 (d, J = 1.8 Hz, 9H). ^{13}C NMR (101 MHz, DMSO) δ 167.69, 162.74, 156.25, 151.31, 142.01, 131.87, 129.73, 127.34, 126.49, 109.49, 35.28, 31.25, 30.22, 28.83, 27.89. HRMS (ESI): calcd for: $C_{19}H_{21}NO_3S$, *m/z* $[M + H]^+$ 343.1242, found 343.1247.

3.2.27. 2-(4-fluorobenzamido)-5,6,7,8-tetrahydro-4H-cyclohepta[b]thiophene-3-carboxylic acid (6i)

White solid; Yield 58.8 %; M.p. 295.3–296.3 °C. ^{1}H NMR (500 MHz, DMSO- d_6) δ 14.01 (s, 1H), 8.17 – 7.17 (m, 4H), 2.89 – 2.61 (m, 2H), 1.81 (p, J = 5.6 Hz, 2H), 1.56 (dp, J = 30.7, 5.4 Hz, 4H). ^{13}C NMR (126 MHz, DMSO) δ 169.58, 165.79(d, J = 2.9 Hz, 1F), 163.80, 161.43, 142.77, 138.41, 130.20, 130.12, 116.52, 116.35, 32.72, 28.79, 28.33, 27.58. HRMS (ESI): calcd for: $C_{17}H_{16}FNO_3S$, *m/z* $[M + H]^+$ 333.0835, found 333.0838.

3.2.28. 2-benzamido-5,6,7,8-tetrahydro-4H-cyclohepta[b]thiophene-3-carboxylic acid (6j)

White solid; Yield 59.1 %; M.p. 298.1–299.1 °C. ^{1}H NMR (500 MHz, DMSO- d_6) δ 14.04 (s, 1H), 8.26 – 7.36 (m, 5H), 2.84 – 2.63 (m, 2H), 1.82 (p, J = 5.7 Hz, 2H), 1.56 (dp, J = 29.9, 5.5 Hz, 4H). ^{13}C NMR (126 MHz, DMSO) δ 169.63, 162.35, 142.46, 138.53, 133.39, 132.58, 129.60, 129.42, 127.45, 118.77, 116.28, 32.76, 28.82, 28.37, 27.63, 27.59. HRMS (ESI): calcd for: $C_{17}H_{17}NO_3S$, *m/z* $[M + H]^+$ 315.0929, found 315.0924.

3.2.29. 2-(2,6-difluorobenzamido)-5,6,7,8-tetrahydro-4H-cyclohepta[b]thiophene-3-carboxylic acid(6 k)

White solid; Yield 55.8 %; M.p. 299.4–300.4 °C. ^{1}H NMR (500 MHz, DMSO- d_6) δ 13.42 (s, 1H), 11.80 (s, 1H), 7.84 – 7.07 (m, 3H), 2.84 – 2.56 (m, 2H), 1.81 (p, J = 5.7 Hz, 2H), 1.61 – 1.30 (m, 4H). ^{13}C NMR (126 MHz, DMSO) δ 167.19, 158.87(m, J = 10.1 Hz, 2F), 156.63, 142.37, 137.55, 134.18, 131.56, 115.79, 113.19, 112.99, 32.32, 28.48, 28.00, 27.73, 27.22. HRMS (ESI): calcd for: $C_{17}H_{15}F_2NO_3S$, *m/z* $[M + H]^+$ 351.0741, found 351.0748.

3.2.30. 2-(3-fluorobenzamido)-5,6,7,8-tetrahydro-4H-cyclohepta[b]thiophene-3-carboxylic acid(6 l)

White solid; Yield 58.1 %; M.p. 305.2–306.2 °C. ^{1}H NMR (500 MHz, DMSO- d_6) δ 12.54 (s, 1H), 7.89 – 7.21 (m, 4H), 2.81 – 2.61 (m, 2H), 1.81 (t, J = 5.8 Hz, 2H), 1.56 (dt, J = 25.4, 5.4 Hz, 4H). ^{13}C NMR (126 MHz, DMSO) δ 168.21, 163.69(d, J = 7.4 Hz, 1F), 161.73, 144.06, 137.65, 135.28, 131.90, 130.94, 123.36, 120.01, 115.51, 114.59, 32.38, 28.55, 28.05, 27.73, 27.25. HRMS (ESI): calcd for: $C_{17}H_{16}FNO_3S$, *m/z* $[M + H]^+$ 333.0835, found 333.0837.

3.2.31. 2-(4-(tert-butyl)benzamido)-5,6,7,8-tetrahydro-4H-cyclohepta[b]thiophene-3-carboxylic acid(6 m)

White solid; Yield 62.1 %; M.p. 301.8–302.8 °C. ^{1}H NMR (500 MHz, DMSO- d_6) δ 13.47 (s, 1H), 12.25 (s, 1H), 7.72 (dd, J = 105.7, 8.1 Hz, 4H), 2.81 – 2.59 (m, 2H), 1.80 (p, J = 5.5 Hz, 2H), 1.58 (dq, J = 18.5, 5.2 Hz, 4H), 1.31 (s, 9H). ^{13}C NMR (126 MHz, DMSO) δ 168.15, 162.89, 156.15, 145.09, 137.31, 130.68, 129.98, 127.32, 126.48, 114.19, 35.27, 32.33, 31.26, 28.48, 28.03, 27.79, 27.20. HRMS (ESI): calcd for: $C_{21}H_{25}NO_3S$, *m/z* $[M + H]^+$ 371.1555, found 371.1550.

3.2.32. 2-((4-(tert-butyl)phenyl)sulfonamido)-4,5,6,7-tetrahydrobenzo[b]thiophene-3-carboxylic acid(6n)

White solid; Yield 58.2 %; M.p. 298.7–299.7 °C. ^{1}H NMR (500 MHz,

DMSO- d_6) δ 7.70 (dd, J = 81.7, 8.2 Hz, 4H), 2.75 – 2.51 (m, 4H), 1.98 – 1.54 (m, 4H), 1.28 (d, J = 7.3 Hz, 9H). ^{13}C NMR (126 MHz, DMSO) δ 166.80, 157.24, 145.88, 136.31, 132.80, 127.38, 127.19, 126.91, 116.60, 35.43, 31.23, 31.14, 26.27, 24.33, 22.85, 22.42. HRMS (ESI): calcd for: $C_{19}H_{23}NO_4S_2$, m/z $[M + H]^+$ 393.1068, found 393.1064.

3.2.33. 2-((3-chlorophenyl)sulfonamido)-4,5,6,7-tetrahydrobenzo[b] thiophene-3-carboxylic acid ***(6o)***

White solid; Yield 66.3 %; M.p. 209.5–210.5 °C. ^{1}H NMR (500 MHz, DMSO- d_6) δ 7.98 – 7.31 (m, 4H), 2.59 (d, J = 6.0 Hz, 4H), 1.66 (dq, J = 18.6, 4.8 Hz, 4H). ^{13}C NMR (126 MHz, DMSO) δ 165.75, 143.46, 141.30, 134.39, 133.86, 133.20, 131.92, 129.15, 126.87, 126.07, 120.09, 26.17, 24.44, 22.84, 22.42. HRMS (ESI): calcd for: $C_{15}H_{14}ClNO_4S_2$, m/z $[M + H]^+$ 371.0053, found 371.0058.

3.2.34. 2-((4-(trifluoromethyl)phenyl)sulfonamido)-4,5,6,7-tetrahydrobenzo[b]thiophene-3-carboxylic acid ***(6p)***

White solid; Yield 58.3 %; M.p. 205.1–206.1 °C. ^{1}H NMR (500 MHz, DMSO- d_6) δ 8.00 (q, J = 8.3 Hz, 4H), 2.57 (dt, J = 14.8, 7.6 Hz, 4H), 1.82 – 1.26 (m, 4H). ^{13}C NMR (126 MHz, DMSO) δ 165.62, 143.55, 133.26, 133.17, 129.26, 128.31, 127.14, 127.11, 127.08, 127.05, 120.34(d, J = 187 Hz, 3F), 26.15, 24.45, 22.84, 22.42. HRMS (ESI): calcd for: $C_{16}H_{14}F_3NO_4S_2$, m/z $[M + H]^+$ 405.0316, found 405.0319.

3.2.35. 2-((2-chlorophenyl)sulfonamido)-4,5,6,7-tetrahydrobenzo[b] thiophene-3-carboxylic acid ***(6q)***

White solid; Yield 60.7 %; M.p. 201.6–202.6 °C. ^{1}H NMR (500 MHz, DMSO- d_6) δ 8.17 – 7.40 (m, 4H), 2.59 (d, J = 5.6 Hz, 4H), 1.63 (dp, J = 12.6, 5.5 Hz, 4H). ^{13}C NMR (126 MHz, DMSO) δ 166.74, 135.67, 132.83, 132.50, 132.10, 130.98, 128.27, 26.26, 24.26, 22.85, 22.41. HRMS (ESI): calcd for: $C_{15}H_{14}ClNO_4S_2$, m/z $[M + H]^+$ 371.0053, found 371.0058.

3.2.36. 2-((4-nitrophenyl)sulfonamido)-4,5,6,7-tetrahydrobenzo[b] thiophene-3-carboxylic acid ***(6r)***

Brown solid; Yield 55.2 %; M.p. 202.8–203.8 °C. ^{1}H NMR (500 MHz, DMSO- d_6) δ 8.22 (dd, J = 177.2, 8.4 Hz, 4H), 2.57 (d, J = 5.7 Hz, 4H), 1.79 – 1.52 (m, 4H). ^{13}C NMR (126 MHz, DMSO) δ 165.36, 150.47, 145.13, 133.40, 129.87, 129.00, 128.95, 125.13, 121.29, 26.12, 24.48, 22.83, 22.41. HRMS (ESI): calcd for: $C_{15}H_{14}N_2O_6S_2$, m/z $[M + H]^+$ 382.0293, found 382.02947.

3.2.37. 2-((4-chlorophenyl)sulfonamido)-4,5,6,7-tetrahydrobenzo[b] thiophene-3-carboxylic acid ***(6 s)***

White solid; Yield 56.7 %; M.p. 210.1–211.1 °C. ^{1}H NMR (500 MHz, DMSO- d_6) δ 7.74 (dd, J = 72.8, 8.2 Hz, 4H), 2.58 (dd, J = 13.0, 7.3 Hz, 4H), 1.84 – 1.56 (m, 4H). ^{13}C NMR (126 MHz, DMSO) δ 165.95, 143.93, 138.87, 138.17, 133.13, 130.07, 129.28, 128.89, 119.46, 26.18, 24.43, 22.84, 22.42. HRMS (ESI): calcd for: $C_{15}H_{14}ClNO_4S_2$, m/z $[M + H]^+$ 371.0053, found 371.0056.

3.2.38. 2-((4-methoxyphenyl)sulfonamido)-4,5,6,7-tetrahydrobenzo[b] thiophene-3-carboxylic acid ***(6 t)***

White solid; Yield 57.8 %; M.p. 207.3–208.3 °C. ^{1}H NMR (500 MHz, DMSO- d_6) δ 7.43 (dd, J = 324.7, 8.7 Hz, 4H), 3.82 (s, 3H), 2.64 (s, 4H), 1.82 – 1.54 (m, 4H). ^{13}C NMR (126 MHz, DMSO) δ 166.58, 132.74, 129.57, 115.11, 56.22, 26.28, 24.37, 22.90, 22.47. HRMS (ESI): calcd for: $C_{16}H_{17}NO_5S_2$, m/z $[M + H]^+$ 367.0548, found 367.0543.

3.2.39. 2-((4-fluorophenyl)sulfonamido)-4,5,6,7-tetrahydrobenzo[b] thiophene-3-carboxylic acid ***(6u)***

White solid; Yield 57.9 %; M.p. 206.8–207.8 °C. ^{1}H NMR (400 MHz, DMSO- d_6) δ 10.78 (s, 1H), 8.08 – 7.25 (m, 4H), 2.60 (s, 4H), 1.66 (dt, J = 12.0, 6.7 Hz, 4H). ^{13}C NMR (101 MHz, DMSO) δ 166.11(d, J = 3.2 Hz, 1F), 163.95, 144.08, 135.48, 133.07, 130.55, 130.46, 128.77, 119.11, 117.28, 117.05, 26.18, 24.40, 22.83, 22.41. HRMS (ESI): calcd for: $C_{15}H_{14}FNO_4S_2$, m/z $[M + H]^+$ 355.0348, found 355.0343.

3.2.40. 2-((5-chlorothiophene)-2-sulfonamido)-4,5,6,7-tetrahydrobenzo [b]thiophene-3-carboxylic acid ***(6v)***

Brown solid; Yield 50.2 %; M.p. 202.1–203.1 °C. ^{1}H NMR (500 MHz, DMSO- d_6) δ 12.40 – 12.17 (s, 1H), 7.70 – 7.05 (m, 4H), 2.66 (dd, J = 56.2, 5.8 Hz, 4H), 1.72 (q, J = 7.5 Hz, 4H). ^{13}C NMR (126 MHz, DMSO) δ 168.00, 162.32, 156.83, 146.15, 135.62, 133.59, 131.77, 128.90, 126.91, 113.34, 26.29, 24.25, 23.00. HRMS (ESI): calcd for: $C_{13}H_{12}ClNO_4S_3$, m/z $[M + H]^+$ 376.9617, found 377.9611.

3.3. In vitro antibacterial activity assay

Bacterial suspensions of *Staphylococcus aureus* (ATCC 25923), *Escherichia coli* (ATCC 25922), *Pseudomonas aeruginosa* (ATCC 27853), and *Salmonella* (ATCC 12022) were transferred to a fresh medium and incubated overnight for further cultivation. The following day, the bacterial solution was diluted to a concentration of 2 × 10^6 colony-forming units per ml and transferred onto a 96-well cell culture plate. Each well was filled with a final volume of 200 μl, comprising a combination of 100 μl of bacterial cell suspension and varying concentrations of target compounds. After a 12-hour incubation period, the viability of the bacteria was assessed using the MTT assay. The MTT reagent (Aladdin China) was added to each well at a final concentration of 1 mg/ml and incubated at 37 °C in the absence of light for a duration of three hours. Then, the formazan crystals were dissolved in DMSO and color development was monitored at a wavelength of 590 nm using a microplate reader (BS1000 Spectra Count, Packard Bioscience Co., Meridien, CT). The experiment was repeated three times.

3.4. Constant concentration time–kill curves

Staphylococcus aureus, *Escherichia coli*, *Pseudomonas aeruginosa*, and *Salmonella* strains were cultivated in LB liquid medium at a temperature of 37 °C and agitated at a rate of 180 rpm in a shaking incubator. The bacterial solution was subsequently diluted to achieve a concentration of approximately 6 × 10^5 colony-forming units per milliliter (CFU/ml). Aliquots of fresh medium were inoculated with resuspended bacteria and a final concentration of test compound **6p** at either 0.5 × MIC, 1 × MIC, or 2 × MIC, respectively. Samples of 0.1 ml were collected at specific time intervals (2, 4, 6, 8, 10, 12, and 24 h) following inoculation. The optical density of each sample was measured using an enzyme plate analyzer. The experimental results were quantified in terms of OD_{600} values, and the experiment was conducted in triplicate.

3.5. Cytotoxicity assay

Cytotoxicity was assessed by employing the Cell Counting Kit-8 (CCK-8, Zeta Life, CA, USA). Briefly, a population of human normal hepatocytes (1 × 10^4 cells per well) were seeded in 96-well plates and incubated for a duration of 24 h. Exponentially proliferating cells were subsequently co-cultured with varying concentrations of compounds for a duration of 48 h, after which 10 μl of CCK-8 reagent was added. After an additional incubation period of 3 h, the absorbance at a specific wavelength of 450 nm was quantified using a microplate reader (SpectraMax i3x, Molecular Devices, USA). The cytotoxic IC_{50} value was calculated from the dose–response curve with the aid of GraphPad Prism software.

3.6. Molecular docking

The Schrödinger software was employed for molecular docking, utilizing the protein preparation module to construct and optimize target proteins. The crystal structure of Salmonella typhimurium (PDB ID: 3B60) was acquired from the Protein Data Bank. All water molecules within the protein were eliminated, and the docking parameters were

adjusted to their default settings.

3.7. Wound-healing assay

In this study, SPF grade male Kunming mice (20–25 g in weight, about 6 weeks old) were provided by the experimental animals of the Army Medical University. The indoor air was fresh, 75 % ± 5 % relative humidity, and the temperature is appropriate. Water and feed are provided free of charge (Shenyang Changsheng provides standard pellet feed). All the experimental animals were observed for one week, and the follow-up test was conducted after there was no death or mental disorder. All animal experiments were approved by the institutional animal care and use Committee of the Army Medical University. The 7-week-old mice were randomly divided into control group and experimental group (every 5 mice were divided into an experimental group, and five parallel experiments were carried out on the experimental group with the same concentration). All surgical instruments must undergo pre-disinfection procedures. The ruler and marker underwent a 30-minute exposure to ultraviolet light prior to their utilization. Mice, aged between 6 and 8 weeks, were subjected to anesthesia and their backs were treated with depilatory cream prior to shaving. Two symmetrical circular wounds, each measuring 5 mm in diameter, were created on the dorsal region of each mouse using a punch tool. A microinjector was utilized to administer the drug to the wound site, whereas the control group was administered a saline solution (20 μl). The test drug concentration of 250 μg/ml was administered on alternate days. The measurement of the wound area was conducted on days 1, 3, 5, 7, and 9 following the treatment.

4. Conclusion

In this study, a total of 40 tetrahydrobenzothiophene derivatives were designed and synthesized. We evaluated their bactericidal activity against bacteria and the results revealed that the majority of these compounds exhibited significant bactericidal activity against bacterial growth. Particularly noteworthy were compounds **6n**, **6o**, **6p**, **6r**, and **6 s**, which displayed remarkable bactericidal activity against both gram-negative and gram-positive bacteria. Of special interest, the time-kill curves of compound **6p** exhibited concentration-dependent antibacterial effects across a range of concentrations. Building on these promising results from cytotoxicity and *in vitro* antibacterial experiments, we selected compound **6p** for molecular simulation docking to further validate its antibacterial activity. The molecular docking results demonstrated that compound 6p displayed a robust affinity for the target protein, establishing strong chemical interactions with Tyr-351, Asp-117, and Tyr-393, forming tightly bound interactions. Furthermore, we established a mouse wound model to investigate the in vivo antibacterial activity of compound **6p**, and our findings revealed that compound **6p** possessed wound healing properties in mice. In a broader context, compound **6p** holds promise as an innovative fungicide for the treatment of bacterial infections.

Funding

This research was funded by the Scientific Technological Research Program of Chongqing Municipal Education Commission (No. KJQN201901501), the National Natural Science Foundation of China (NSFC, No. 82173764), the major project of Study on Pathogenesis and Epidemic Prevention Technology System (No. 2021YFC2302500), the Natural Science Foundation of Chongqing (cstc2021jcyj-msxmX0136, CSTB2022NSCQ-MSX0474), and the Postgraduate Innovation Program of Chongqing University of Science and Technology (No. YKJCX2320510).

Declaration of Competing Interest

The authors declare that they have no known competing financial interests or personal relationships that could have appeared to influence the work reported in this paper.

Appendix A. Supplementary data

Supplementary data to this article can be found online at https://doi.org/10.1016/j.bioorg.2023.106932.

References

[1] L. Serwecińska, Antimicrobials and antibiotic-resistant bacteria: a risk to the environment and to public health, Water 12 (12) (2020) 3313, https://doi.org/10.3390/w12123313.
[2] H.V. Espinoza, J.L. Espinoza, Emerging superbugs: the threat of carbapenem resistant enterobacteriaceae, AIMS Microbiol. 6 (3) (2020) 176, https://doi.org/10.3934/microbiol.2020012.
[3] M.S. Butler, M.A.T. Blaskovich, M.A. Cooper, Antibiotics in the clinical pipeline at the end of 2015, J. Antibiot. 70 (1) (2017) 3–24. https://doi-org.ezproxy.is.ed.ac.uk/10.1038/ja.2016.72.
[4] T.J. Foster, Antibiotic resistance in Staphylococcus aureus current status and future prospects, FEMS Microbiol. Rev. 41 (3) (2017) 430–449. https://doi-org.ezproxy.is.ed.ac.uk/10.1093/femsre/fux007.
[5] B.H. Nataraj, R.H. Mallappa, Antibiotic resistance crisis: an update on antagonistic interactions between probiotics and methicillin-resistant staphylococcus aureus (MRSA), Curr. Microbiol. 78 (6) (2021) 2194–2211. https://doi-org.ezproxy.is.ed.ac.uk/10.1007/s00284-021-02442-8.
[6] J. Vila, J. Moreno-Morales, C. Ballesté-Delpierre, Current landscape in the discovery of novel antibacterial agents, Clinical Microbiol. Infection 26 (5) (2020) 596–603, https://doi.org/10.1016/j.cmi.2019.09.015.
[7] E.D. Brown, G.D. Wright, Antibacterial drug discovery in the resistance era, Nature 529 (7586) (2016) 336–343. https://doi-org.ezproxy.is.ed.ac.uk/10.1038/nature17042.
[8] H. Wang, D. Chen, H. Lu, Anti-bacterial monoclonal antibodies: next generation therapy against superbugs, Applied Microbiology Biotechnology 106 (11) (2022) 3957–3972. https://doi-org.ezproxy.is.ed.ac.uk/10.1007/s00253-022-11989-w.
[9] T. Velkov, K.D. Roberts, P.E. Thompson, J. Li, Polymyxins: a new hope in combating Gram-negative superbugs? Future Med. Chem. 8 (10) (2016) 1017–1025. https://doi-org.ezproxy.is.ed.ac.uk/10.4155/fmc-2016-0091.
[10] S. Roy, J. Roy, B. Guo, Nanomaterials as multimodal photothermal agents (PTAs) against 'Superbugs', J. Mater. Chem. B 11 (11) (2023) 2287–2306. https://doi-org.ezproxy.is.ed.ac.uk/10.1039/D2TB02396B.
[11] X. Li, H. Bai, Y. Yang, J. Yoon, S. Wang, X. Zhang, Supramolecular antibacterial materials for combatting antibiotic resistance, Adv. Mater. 31 (5) (2019) 1805092. https://doi-org.ezproxy.is.ed.ac.uk/10.1002/adma.201805092.
[12] L.D. Högberg, A. Heddini, O. Cars, The global need for effective antibiotics: challenges and recent advances, Trends Pharmacol. Sci. 31 (11) (2010) 509–515. https://doi-org.ezproxy.is.ed.ac.uk/10.1016/j.tips.2010.08.002.
[13] E. Martens, A.L. Demain, The antibiotic resistance crisis, with a focus on the United States, J. Antibiot. 70 (5) (2017) 520–526. https://doi-org.ezproxy.is.ed.ac.uk/10.1038/ja.2017.30.
[14] S. Mitra, S.A. Sultana, S.R. Prova, T.M. Uddin, F. Islam, R. Das, F. Nainu, S. Sartini, K. Chidambaram, F.A. Alhumaydhi, Investigating forthcoming strategies to tackle deadly superbugs: current status and future vision, Expert Rev. Anti Infect. Ther. 20 (10) (2022) 1309–1332. https://doi-org.ezproxy.is.ed.ac.uk/10.1080/14787210.2022.2122442.
[15] R. Vivas, A.A.T. Barbosa, S.S. Dolabela, S. Jain, Multidrug-resistant bacteria and alternative methods to control them: an overview, Microb. Drug Resist. 25 (6) (2019) 890–908. https://doi-org.ezproxy.is.ed.ac.uk/10.1089/mdr.2018.0319.
[16] J. Jampilek, Design and discovery of new antibacterial agents: Advances, perspectives, challenges, Curr. Med. Chem. 25 (38) (2018) 4972–5006. https://doi-org.ezproxy.is.ed.ac.uk/10.2174/0929867324666170918122633.
[17] N. Jackson, L. Czaplewski, L.J. Piddock, Discovery and development of new antibacterial drugs: learning from experience? J. Antimicrob. Chemother. 73 (6) (2018) 1452–1459. https://doi-org.ezproxy.is.ed.ac.uk/10.1093/jac/dky019.
[18] U. Theuretzbacher, E. Baraldi, F. Ciabuschi, S. Callegari, Challenges and shortcomings of antibacterial discovery projects, Clinical Microbiology Infection 29 (5) (2023) 610–615, https://doi.org/10.1016/j.cmi.2022.11.027.
[19] K. Bush, P.A. Bradford, Interplay between β-lactamases and new β-lactamase inhibitors, Nat. Rev. Microbiol. 17 (5) (2019) 295–306. https://doi-org.ezproxy.is.ed.ac.uk/10.1038/s41579-019-0159-8.
[20] C.L. Tooke, P. Hinchliffe, E.C. Bragginton, C.K. Colenso, V.H. Hirvonen, Y. Takebayashi, J. Spencer, β-Lactamases and β-Lactamase Inhibitors in the 21st Century, J. Mol. Biol. 431 (18) (2019) 3472–3500, https://doi.org/10.1016/j.jmb.2019.04.002.
[21] E. Culp, G.D. Wright, Bacterial proteases, untapped antimicrobial drug targets, J. Antibiot. 70 (4) (2017) 366–377. https://doi-org.ezproxy.is.ed.ac.uk/10.1038/ja.2016.138.

[22] N. Nawaz, S. Wen, F. Wang, S. Nawaz, J. Raza, M. Iftikhar, M. Usman, Lysozyme and its application as antibacterial agent in food industry, Molecules 27 (19) (2022) 6305, https://doi.org/10.3390/molecules27196305.
[23] M.J. Lasko, D.P. Nicolau, Carbapenem-resistant enterobacterales: considerations for treatment in the era of new antimicrobials and evolving enzymology, Curr. Infect. Dis. Rep. 22 (3) (2020) 6. https://doi-org.ezproxy.is.ed.ac.uk/10.1007/s11908-020-0716-3.
[24] S. Hawser, S. Lociuro, K. Islam, Dihydrofolate reductase inhibitors as antibacterial agents, Biochem. Pharmacol. 71 (7) (2006) 941–948, https://doi.org/10.1016/j.bcp.2005.10.052.
[25] W. Li, F. Separovic, N.M. O'Brien-Simpson, J.D. Wade, Chemically modified and conjugated antimicrobial peptides against superbugs, Chem. Soc. Rev. 50 (8) (2021) 4932–4973. https://doi-org.ezproxy.is.ed.ac.uk/10.1039/D0CS01026J.
[26] U. Theuretzbacher, K. Bush, S. Harbarth, M. Paul, J.H. Rex, E. Tacconelli, G. E. Thwaites, Critical analysis of antibacterial agents in clinical development, Nat. Rev. Microbiol. 18 (5) (2020) 286–298. https://doi-org.ezproxy.is.ed.ac.uk/10.1038/s41579-020-0340-0.
[27] D.E. Nawrot, G. Bouz, O. Janďourek, K. Konečná, P. Paterová, P. Bárta, M. Novák, R. Kučera, J. Zemanová, M. Forbak, Antimycobacterial pyridine carboxamides: from design to in vivo activity, Eur. J. Med. Chem. 258 (2023), 115617, https://doi.org/10.1016/j.ejmech.2023.115617.
[28] P. Chen, J. Yang, Y. Zhou, X. Li, Y. Zou, Z. Zheng, M. Guo, Z. Chen, W.-J. Cho, N. Chattipakorn, Design, synthesis, and bioactivity evaluation of novel amide/sulfonamide derivatives as potential anti-inflammatory agents against acute lung injury and ulcerative colitis, Eur. J. Med. Chem. 259 (2023), 115706, https://doi.org/10.1016/j.ejmech.2023.115706.
[29] F.A. Thélot, W. Zhang, K. Song, C. Xu, J. Huang, M. Liao, Distinct allosteric mechanisms of first-generation MsbA inhibitors, Science 374 (6567) (2021) 580–585, https://doi.org/10.1126/science.abi9009.
[30] L. Lai, J. Yang, W. Sun, X. Su, J. Chen, X. Chen, S. Pei, Design, synthesis and antibacterial evaluation of a novel class of tetrahydrobenzothiophene derivatives, RSC Medicinal Chemistry 14 (1) (2023) 166–172. https://doi-org.ezproxy.is.ed.ac.uk/10.1039/D2MD00373B.
[31] S. Pei, J. Yang, S. Xia, S. Tang, K. Yuan, J. Chen, Design synthesis, and antibacterial evaluation of tetrahydrobenzothiophene derivatives as lipopolysaccharide biogenesis inhibitors, Letters in Drug Design & Discovery 20 (03) (2023) 335–342. https://doi-org.ezproxy.is.ed.ac.uk/10.2174/1570180819666220317151208.
[32] G. Zhang, V. Baidin, K.S. Pahil, E. Moison, D. Tomasek, N.S. Ramadoss, A. K. Chatterjee, C.W. McNamara, T.S. Young, P.G. Schultz, T.C. Meredith, D. Kahne, Cell-based screen for discovering lipopolysaccharide biogenesis inhibitors, Proc. Natl. Acad. Sci. 115 (26) (2018) 6834–6839. https://doi-org.ezproxy.is.ed.ac.uk/10.1073/pnas.1804670115.